View Online
Dynamic Article Links

Dalton Transactions

Cite this: *Dalton Trans.*, 2011, **40**, 5781

www.rsc.org/dalton

PAPER

Pt(II) complexes with bidentate and tridentate pyrazolyl-containing chelators: synthesis, structural characterization and biological studies†

Carla Francisco,[a] Sofia Gama,[a] Filipa Mendes,[a] Fernanda Marques,[a] Isabel Cordeiro dos Santos,[a] António Paulo,[a] Isabel Santos,[a] Joana Coimbra,[b] Elisabetta Gabano[c] and Mauro Ravera*[c]

Received 16th December 2010, Accepted 24th March 2011
DOI: 10.1039/c0dt01785j

A series of four Pt(II) complexes anchored by bidentate or tridentate pyrazolyl-alkylamine chelators bearing different substituents at the azolyl rings has been prepared with the aim to assess their interest in the design of novel anticancer drugs. All complexes have been fully characterized by classical analytical methods and three of them were characterized also by X-ray diffraction analysis. Their solution behavior, together with lipophilicity measurements, cell uptake, antiproliferative properties, DNA interaction have been evaluated. Albeit all the complexes were less active than cisplatin on ovarian carcinoma A2780 cell line, greatly retained their activity in the cisplatin-resistant A2780cisR cell line and presented a lower resistance factor compared to cisplatin. Moreover, the Pt(II) complexes under investigation were less prone to undergo deactivation by glutathione, believed to be the major cellular target of cisplatin that inactivates the drug by binding to it irreversibly.

Introduction

Cisplatin (*cis*-diamminedichloridoplatinum(II), *cis*-[$PtCl_2(NH_3)_2$]) and succeeding platinum derivatives such as carboplatin and oxaliplatin play an important role in the treatment of certain human cancers, being used routinely and worldwide in the standard treatment of solid tumours.[1] In particular, cisplatin is approved by the Food and Drug Administration (FDA) to be used by itself or together with other drugs to treat bladder, ovarian, testicular cancers, locally advanced squamous cell carcinoma of the head and neck (SCCHN), late-stage cervical cancer, malignant mesothelioma, and non-small cell lung cancer (NSCLC).[2] It has been estimated that as many as 50–70% of cancer patients are treated with a platinum drug.[3]

For instance, in the case of testicular cancer, the development of cisplatin-based combination chemotherapy such as PVB (cisplatin, vinblastin and bleomycin) therapy in the late 1970s resulted in a dramatic improvement in the prognosis of patients, and overall cure rates now exceed 80%.[4]

On the contrary, the prognosis for women with ovarian cancer can be defined by the tumor response to cisplatin: patients whose tumors are naturally platinum-resistant at the time of initial treatment have a very poor prognosis. Sadly, albeit the majority of patients with ovarian cancer respond to front-line platinum combination chemotherapy, also in this case the greater part is destined to develop resistance to cisplatin.[5]

More generally, the use of cisplatin has serious disadvantages, namely severe toxic side effects which often limit the amount of drug that can be administered. For these reasons, the development of new and more efficient antitumor-active platinum compounds still remains an important topic of research in biomedical inorganic chemistry.

In the case of square-planar Pt(II) complexes, an increase in the steric environment around the metal atom can reduce the level of undesired substitution reaction, in particular with proteins.[6] For this reason, the presence of the sterically demanding 2-methylpyridine (2-picoline) in the coordination sphere of Pt(II) metal centre render the *cis*-amminedichlorido(2-methylpyridine)platinum(II) (picoplatin) able to circumvent the cellular resistance mechanism.[7] The efficacy of picoplatin to overcome platinum resistance in patients with platinum-refractory/-resistant small-cell lung cancer (SCLC) was recently demonstrated.[8]

As far as substitution at carbons adjacent to the nitrogen atoms of N-heterocyclic rings is particularly straightforward to achieve, it is possible to strongly affect the steric environment around the N-donor atoms and any metal ions coordinated to them. Dimetallic platinum complexes containing bridging pyrazoles as coordinating moieties are other examples of transition metal complexes with N-heterocyclic ligands that have been the subject of recent studies because of their beneficial effects as anticancer agents.[9] In a

[a]*Unidade de Ciências Químicas e Radiofarmacêuticas, ITN, Estrada Nacional 10, 2686-953, Sacavém Codex, Portugal*
[b]*LCA-Laboratório Central de Análises, Universidade de Aveiro, 3810-193, Aveiro, Portugal*
[c]*Dipartimento di Scienze dell'Ambiente e della Vita, Università del Piemonte Orientale "Amedeo Avogadro", Viale Michel 11, 15100, Alessandria, Italy. E-mail: mauro.ravera@mfn.unipmn.it; Fax: +39 0131 360250*

† CCDC reference numbers **5** (CCDC reference number CCDC 805451), **6** (CCDC 805452), and **12** (CCDC 805453). For crystallographic data in CIF or other electronic format see DOI: 10.1039/c0dt01785j

different approach, tridentate pyrazolyl-containing chelators were used to stabilize the *fac*-$[M(CO)_3]^+$ (M = Re, ^{99m}Tc) core to produce radioactive complexes that were evaluated as specific probes for nuclear imaging of a variety of neurologic, cardiac and oncologic diseases or as Auger-emitting radiopharmaceuticals for targeted anti-tumor therapy.[10,11] In particular, ^{99m}Tc(I) tricarbonyl complexes anchored by pyrazolyl-diamine ligands functionalized with polyaromatic DNA intercalators have shown the capability to target the nucleus of murine tumor cells, in some cases with remarkable cell killing at low radioactivity levels and mainly through apoptotic pathways.[11,12] These encouraging findings prompted us to extend the studies to Pt(II) complexes anchored on tridentate pyrazolyl-diamine ligands and on congener bidentate ligands, expecting to obtain new compounds with the ability to accumulate into tumor cells and to induce cytotoxic effects.

This paper will report on the synthesis, characterization and biological evaluation of a small series of Pt(II) compounds anchored by bidentate (pz*N) or tridentate (pz*NN) pyrazolyl-alkylamine chelators bearing different substituents at the azolyl rings (Fig. 1).[13,14] By exploring ligands of different denticity and/or with different substituents at the azolyl rings, we intended to tune the steric environment and lipophilicity of the complexes, which are crucial factors of their ability to enter into neoplasic cells and interact with DNA.

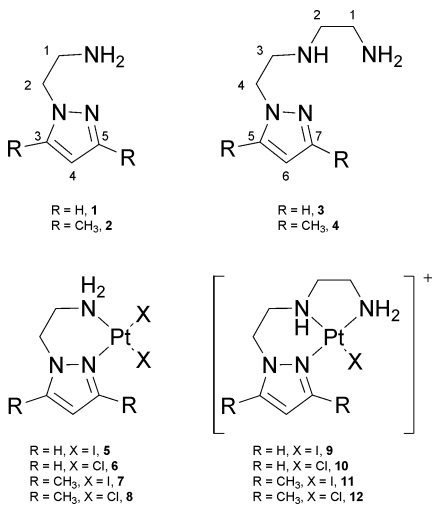

Fig. 1 Sketch of the bidentate (pz*N) and tridentate (pz*NN) pyrazolyl-alkylamine chelators **1–4**, and their Pt(II) complexes **5–12**.

Results and discussion

Synthesis of the complexes with bidentate ligands [Pt(pz*N)X$_2$] (X = I, Cl) 5–8

The Pt(II) compounds with bidentate ligands were synthesized according to a procedure based on Dhara's method.[15,16] Briefly, the reaction between $K_2[PtCl_4]$ and KI produces $K_2[PtI_4]$ in solution; the latter complex reacts with ligands **1** and **2** to give the *cis*-$[Pt(pz*N)I_2]$ precipitate (compounds **5** and **7**). Upon reaction with Ag_2SO_4, the diiodido synthon produces the corresponding diaqua intermediate, which reacts with chlorides to yield the final complex *cis*-$[Pt(pz*N)Cl_2]$ (compounds **6** and **8**) (Scheme 1).

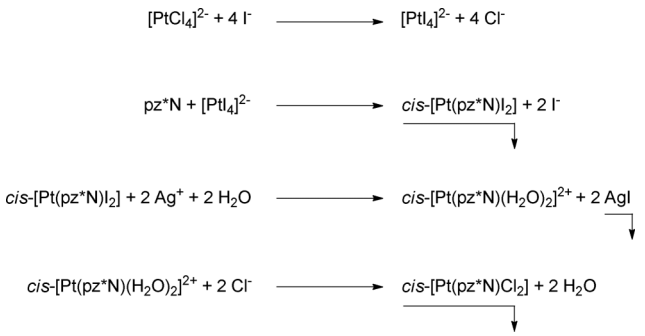

Scheme 1 Scheme of the Dhara's method for the synthesis of Pt-complexes containing bidentate ligands pz*N. All reactions are performed in water.

Synthesis of the complexes with tridentate ligands [Pt(pz*NN)X]X (X = I, Cl) 9–12

The Pt(II) compounds with tridentate ligands were synthesized according to two different procedures (Scheme 2): *i*) an adaptation of the Dhara's method described above,[17] and *ii*) the method described by Annibale *et al.* for [Pt(dien)Cl]Cl (dien = diethylenetriamine).[18] According to the first procedure, the iodido Pt-complex is the synthon for the final chlorido compound. Upon the use of $AgNO_3$, the chlorido complex has a mixture of nitrate and chloride as counter ion (confirmed by ion chromatography). The use of an anion-exchange resin allows getting chloride as final counter ion. On the contrary, according to the second procedure, [Pt(pz*NN)Cl]Cl is obtained in high yield (> 90%) by reaction of *cis*-$[PtCl_2(DMSO)_2]$ (DMSO = dimethylsulfoxide) with pz*NN in methanol. This method proved to be better in terms of purity of the final product for **12**, whereas the Dhara's method was better for **10**.

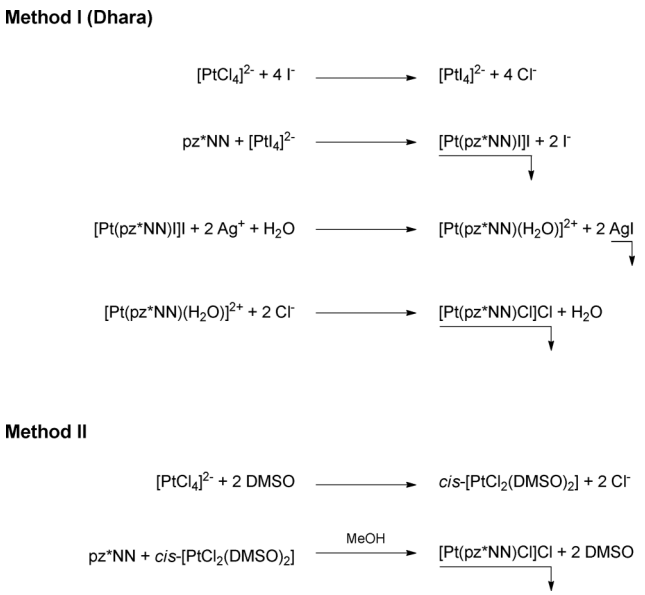

Scheme 2 Scheme of the two procedures for the synthesis of Pt-complexes containing tridentate ligands pz*NN. All reactions are performed in water, except where otherwise indicated.

Characterization of the complexes

The chemical identity of the newly synthesized Pt(II) complexes, **5–12**, was ascertained by electrospray mass spectrometry (ESI-MS) and by multinuclear NMR spectroscopy. The characterization of **5**, **6** and **12** was also done by X-ray diffraction analysis.

For the complexes with the bidentate pzN* ligands, **5–8**, the positive ESI-MS spectra in methanol/DMSO (99 : 1) solutions have shown the presence of peaks corresponding to the solvated species $[Pt(pz*N)(X)(DMSO)]^+$ (X = I, Cl), due to the replacement of one of the coordinated halides by DMSO, as commonly observed for cisplatin-like complexes anchored by diamine ligands. The ESI-MS spectra of **9–12**, anchored by the tridentate pz*NN chelators, were run in methanol/acetone (98 : 2) or methanol–water (98 : 2) solutions, and exhibited peaks corresponding to $[Pt(pz*NN)(X)]^+$ (X = Cl, I), in agreement with the cationic character of these complexes. These peaks displayed isotopic patterns in agreement with the elemental composition of the compounds.

In the ^{1}H NMR spectra of **5–12**, the resonances due to the N–H, methylenic and pyrazolyl protons are downfield shifted compared to the corresponding resonances in the spectra of the respective free ligands, which is consistent with the coordination of the azole rings and aliphatic amine groups of the chelators to the Pt(II) metal centre.

The ^{1}H NMR spectra of **5–8** are rather simple, presenting only two multiplets for the CH_2 protons of the pz–CH_2–CH_2–NH_2 ethylenic chain. Upon coordination to the metal, these protons should become diastereotopic due to expected increasing rigidity of the ligand. In fact, this behaviour has been reported for similar Pt(II) complexes anchored by bidentate N-alkyl substituted pz*N ligands, which have shown four resonances for the diastereotopic CH_2 protons of the pz–CH_2–CH_2–NH(R) ethylenic chain.[19] On the contrary, in complexes **5–8**, the presence of a residual dynamic process involving the six-membered chelate ring produces a partial overlap of the resonances of the two protons belonging to the same CH_2 group.

The ^{1}H NMR spectra of complexes **9–12** display a common pattern. Each CH_2 group from the tridentate pz*NN chelator originates a single resonance integrating for two protons, excepting the CH_2 protons adjacent to the pyrazolyl ring that originate two multiplets with the same intensity, appearing between 4.25 and 5.00 ppm. Although we cannot exclude that there is occasional overlap of some resonances, this pattern seems to indicate that **9–12** undergo dynamic processes that make some of the diastereotopic methylenic protons magnetically equivalent. Apparently, the CH_2 protons adjacent to the azolyl ring are the less affected by those processes, most probably because they are located in the less flexible part of the molecules.

The ^{195}Pt{^{1}H} NMR spectra of freshly prepared solutions of complexes **5–12** exhibited only one signal at chemical shifts that were consistent with the retention of the coordination sphere without involvement of solvation reactions. For the *cis*-diiodido Pt(II) complexes **5** and **7**, these signals appear at –3365 and –3357 ppm, respectively, and are well within the range of values (–3389 to –3198 ppm) reported in the literature for complexes with the $[PtI_2N_2]$ core;[20] the chemical shifts of the ^{195}Pt resonances of the dichlorido congeners **6** (–2261 ppm) and **8** (–2213 ppm) are consistent with a *cis*-$[PtCl_2N_2]$ coordination sphere, being comparable with the values (–2242 to –2009 ppm) found for other Pt(II) complexes presenting the same core.[20] The Pt(II)-chlorido complexes with the pz*NN ligands, **10** and **12**, have shown ^{195}Pt chemical shifts at –2691 and –2657 ppm, respectively, which can be considered compatible with the coordination of a (*N*,*N*′,*N*″)-tridentate pz*NN chelator and a chloride co-ligand, although being lower than the values (–2579 to –2495 ppm) reported for other cationic complexes with the core $[PtClN_3]$.[21] The corresponding Pt(II)-iodido complexes, **9** and **11**, have shown ^{195}Pt resonances at much higher field (–3070 and –3115 ppm, respectively), which reflect the softer character of iodide compared to chloride.[22]

Table 1 Selected bond lengths (Å) and angles (°) for compounds **5**, **6** and **12**

5		**6**	
Pt(1)–N(1)	2.042(8)	Pt(1)–N(1)	2.025(5)
Pt(1)–N(3)	2.081(7)	Pt(1)–N(3)	2.041(5)
Pt(1)–I(1)	2.5973(7)	Pt(1)–Cl(2)	2.2938(16)
Pt(1)–I(2)	2.5807(7)	Pt(1)–Cl(1)	2.3113(16)
N(1)–Pt(1)–N(3)	92.4(3)	N(1)–Pt(1)–N(3)	92.6(2)
N(1)–Pt(1)–I(2)	177.54(19)	N(1)–Pt(1)–Cl(2)	178.72(14)
N(3)–Pt(1)–I(2)	86.6(2)	N(3)–Pt(1)–Cl(2)	86.54(17)
N(1)–Pt(1)–I(1)	91.2(2)	N(1)–Pt(1)–Cl(1)	89.92(14)
N(3)–Pt(1)–I(1)	176.3(2)	N(3)–Pt(1)–Cl(1)	177.50(16)
I(2)–Pt(1)–I(1)	89.82(2)	Cl(2)–Pt(1)–Cl(1)	90.96(6)
12			
Pt(1)–N(1)	2.018(3)	Pt(1)–N(4)	2.028(3)
Pt(1)–N(3)	2.053(3)	Pt(1)–Cl(1)	2.3224(8)
N(1)–Pt(1)–N(4)	173.94(13)	N(1)–Pt(1)–N(3)	90.32(13)
N(4)–Pt(1)–N(3)	84.06(13)	N(1)–Pt(1)–Cl(1)	94.44(10)
N(4)–Pt(1)–Cl(1)	91.21(10)	N(3)–Pt(1)–Cl(1)	175.20(9)

X-ray analysis

X-ray quality crystals were obtained for **5**, **6** and **12**, as described in the experimental section. ORTEP diagrams of the structures of **5** and **6** are presented in Fig. 2 and an ORTEP view of the cation of **12** is shown in Fig. 3. A selection of bond distances and angles are listed in Table 1.

For all the three compounds, the platinum atom is in a slightly distorted square coordination environment, which is defined in the case of **5** and **6** by the two nitrogen atoms from the bidentate pz*N ligands and by two chlorine atoms in a *cis* arrangement, while in the case of **12** is defined by three nitrogen atoms of the tridentate pz*NN chelator and by a chloride co-ligand. The slight distortion can be seen by the *trans* angles around the metal (spanning between 173.94° and 178.12°) and from the deviation of the Pt(II) atom (**5**: 0.0196 Å; **6**: 0.0082 Å; **12**: 0.0066 Å) from the mean plane containing the four coordinated atoms.

In the structures of **5**, **6** and **12**, the Pt–N_{pz} bond distances appear in the range 2.018(3)–2.042(8) Å and the Pt–N_{amine} bond distances span between 2.028 and 2.081 Å. These distances are normal and can be considered comparable to the values reported in the literature for other Pt(II) complexes containing pyrazolyl and/or aliphatic amine donor groups.[19,23] Complex **6** has shown the highest Pt–N bond distances (Pt–N_{pz} = 2.042(8) Å and

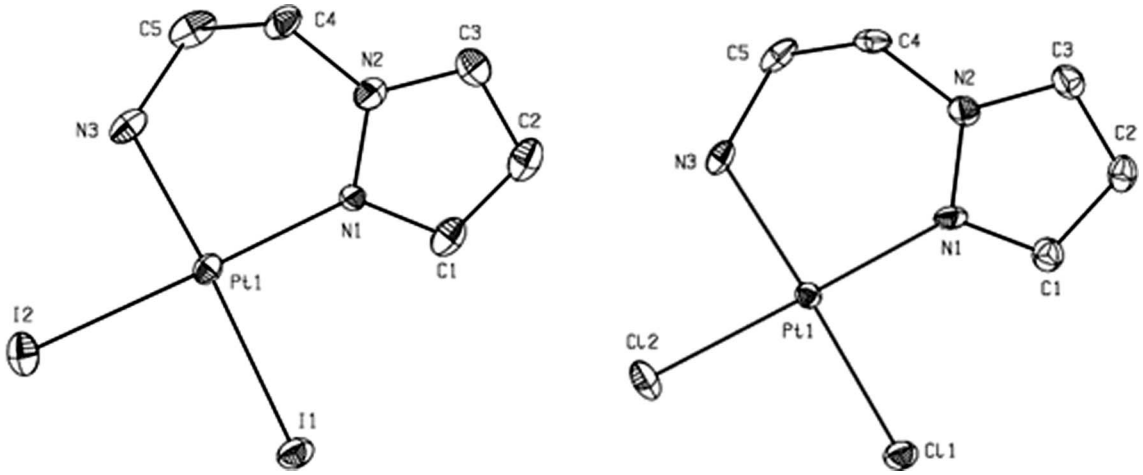

Fig. 2 ORTEP diagrams of complexes **5** (left) and **6** (right); thermal ellipsoids are drawn at the 40% probability level.

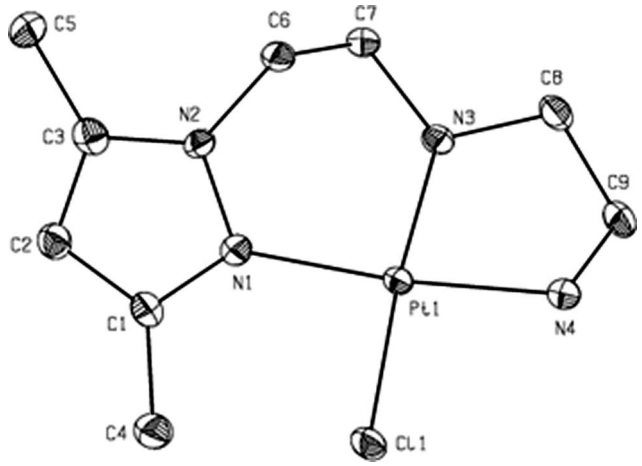

Fig. 3 ORTEP view of the cation of compound **12**; thermal ellipsoids are drawn at the 40% probability level.

Pt–N_{amine} = 2.081(7) Å) as a consequence of the higher *trans* influence of iodide compared to chloride. The Pt–I bond distances in **5** (av. 2.5890(7) Å) and the Pt–Cl bond distances in **6** (av. 2.3026 Å) and **12** (2.3224) are within the range of values found for Pt–X (X = Cl, I) bond lengths in complexes with the $[PtX_2N_2]$ (X = Cl, I) or $[PtClN_3]$ cores.[24]

Solution behavior

Differences in reactivity towards the solvolysis for the complexes under investigation were evaluated by means of conductivity measurements. Conductivity measurements allow determining the electrolytic behavior of a solution and are fit for following the kinetics of the solvolysis of platinum compounds that are converted, also rather quickly, in mono- or di-charged species that rapidly increase the conductivity of the solution.

In order to simulate the conditions used in the cytotoxicity tests, the mother solutions of the complexes **6**, **8**, **10** and **12**, prepared in DMSO, were diluted with ultrapure water to a final 2% of organic co-solvent (0.5 mM complex) and maintained at 37 °C for three days. At selected time intervals, the conductivity of the solution has been measured. For comparison, the same experiment has been performed with cisplatin.

It is known that cisplatin, and in general chlorido-Pt(II) complexes, undergo hydrolysis/solvolysis. The overall reaction pattern is quite complicate, also because strictly depending on the experimental conditions.[25] It has been reported that at physiological pH and at a concentration of 4 mM Cl^- the almost complete hydrolysis of cisplatin occur (half-life of approx 2 h at 37 °C) to give a 50 : 50 mixture of $[PtCl(H_2O)(NH_3)_2]^+$ and $[PtCl(OH)(NH_3)_2]$. The absence of chlorides and the presence of DMSO will increase the solvolysis of the complexes, also with the formation of Pt-DMSO species.[26]

The conductivity of solutions of complexes **6**, **8**, **10** and **12** increases with time. The dichlorido, neutral complexes, **6** and **8**, underwent solvolysis to give mono-charged species, while the monochlorido cationic complexes, **10** and **12**, produced dicationic species. The initial rate of solvolysis are almost the same for the bidentate complexes **6** and **8** ($t_{\frac{1}{2}} \cong 0.2$ h), whereas the tridentate species **10** and **12** have a slower initial rate ($t_{\frac{1}{2}} > 2.8$ h). In all cases, conductivity reached a plateau: for **6** and **8** conductivity plateaued after 6-8 h, while species **10** and **12** reached the plateau over a longer time (>17 h, Table 2).

The conductivity value at the plateau for **6** and **8** was at the lowest end of the range for a 1 : 1 electrolyte. Similarly, the conductivity of **10** and **12** started from the 1 : 1 range and plateaued at the lowest end of the range for a 2 : 1 electrolyte in similar experimental conditions. These results might suggest a partial solvolysis. The methylated compounds show a slower rate of hydrolysis, reflecting the highest steric environment of the complexes.

ESI-MS of the 3-day old solutions confirmed the formation of the solvolysis products, even though, as expected, the solvolysis of the complexes was not complete. For **6** and **8** the main species in the mass spectra was $[M–Cl+DMSO]^+$ (with some amount of $[M–Cl+H_2O]^+$) and the original complexes were still present in low percentage. For **10** and **12** the situation was the opposite: the highest signals were those of the intact complexes and the solvated species had lower intensity. It is important to recall that ESI-MS highlights the presence of the easiest ionizable species, not necessarily the most abundant in solution. Moreover, *in vitro*

Table 2 Kinetic data and partition coefficient

Complex	Initial rate $t_{\frac{1}{2}}$ (h)	Time to reach the plateau (h)	Conductivity at plateau (μS cm^{-1})	miLog*P* of the ligands[a]	log *k*′ of the complexes[b]
6	0.20	6	74	(**1**) −0.81	−0.003
8	0.23	8	71	(**2**) −0.37	0.525
10	2.84	17	123	(**3**) −1.37	−1.057
12	4.48	20	120	(**4**) −0.93	−0.132

[a] Calculated with the tools implemented in Virtual Computational Chemistry Laboratory.[30] miLogP is calculated by the methodology developed by Molinspiration (http://www.molinspiration.com/) as a sum of fragment-based contributions (which have been obtained by fitting calculated log$P_{o/w}$ with experimental log$P_{o/w}$ for a training set containing more than twelve thousand molecules) and correction factors. [b] HPLC capacity factors $k' = (t_R - t_0)/t_0$, where t_0 is the retention time for an unretained compound and t_R is the retention time of the analysed species.

and *in vivo* (*i.e.*, in the presence of buffers like phosphates and carbonates) the solvolysis of the complexes is faster.[27]

HPLC measurements performed on the compounds aged in 2% DMSO/water confirms the general trend observed by conductivity experiments. Also in the case of complexes dissolved in pure water a similar behaviour is observed, albeit with slower solvolysis (aquation) time (for instance, in the case of **6**, $t_{\frac{1}{2}}$ is 1.46 h).

Lipophilicity measurements

The partition coefficient *P* is the ratio between the concentrations of a compound dissolved in two immiscible solvents, usually *n*-octanol and water ($P_{o/w}$). The log$P_{o/w}$ is widely used as an index of molecular lipophilicity of a drug, which is related to its ability to cross cell membranes by means of passive diffusion (n-octanol models the lipidic bilayer of cell membranes and water represents the fluid in and out of cells). Moreover, there is an exponential relationship between log$P_{o/w}$ and cellular uptake.[28]

Since RP-HPLC retention is due to partitioning between the mobile and stationary phases, there is a correlation between partition coefficients and HPLC capacity factors *k*′ ($k' = (t_R - t_0)/t_0$, where t_0 is the retention time for an unretained compound and t_R is the retention time of the analysed species). Therefore, we employed a RP-HPLC method for the evaluation of log *k*′ (aqueous HCOOH/MeOH 80/20, see Experimental) of **6**, **8**, **10**, and **12**.[29] For the sake of comparison, the lipophilicity of the ligands (miLog*P*) has been calculated with the tools implemented in Virtual Computational Chemistry Laboratory (Table 1).[30]

All complexes but **10** are less hydrophilic than cisplatin (log $k' = -0.605$) in the order **10** < **12** < **6** < **8** (*i.e.*, charged, tridentate < neutral, bidentate complexes). As expected, complexes with methylated ligands are more lipophilic than non-methylated analogues (**8** *vs.* **6**, and **12** *vs.* **10**).

Interestingly, the observed order of lipophilicity of the complexes is the same calculated for the corresponding ligands (*i.e.*, **3** < **4** < **1** < **2**). This finding seems to suggest that the contribution of the "PtCl$_n$" moiety is to some extent additive, despite the difference in the nature of the metal fragment, and does not alter significantly the trend of lipophilicity values of the ligands. A strict additive effect was already observed for other Pt-containing molecules,[31] but in that case the Pt-fragment was exactly the same. Many of the methods developed for the calculation of log$P_{o/w}$ from molecular structure are based on the Hansch fragmental approach, where the lipophilicity of the whole molecule is obtained by adding to the lipophilicity its fragments.[32]

Table 3 IC_{50} values for 72 h continuous treatment of two different human tumour cell lines (A2780 ovarian carcinoma and its cisplatin-resistant variant A2780cisR) with compounds **6**, **8**, **10** and **12** and the reference complex cisplatin

	IC_{50} (μM)				
Complex	A2780	A2780cisR	A2780cisR +BSO[a]	*RF*[b]	*MF*[c]
6	10 ± 0.9	29 ± 3.6	19 ± 6.5	2.9	1.5
8	32 ± 4.6	40 ± 6	14 ± 1.0	1.3	2.9
10	152 ± 15	207 ± 145	79 ± 24	1.4	2.6
12	35 ± 8	40 ± 8	19 ± 4	1.1	2.1
Cisplatin	2.5 ± 0.3	14 ± 2.2	3.1 ± 0.6	5.6	4.5

[a] +BSO indicates that the cells were first pre-incubated for 2 h with 400 μM BSO in order to deplete cellular GSH levels. Pt complexes were incubated for 72 h in the presence of 25 μM BSO. [b] Resistance Factor (*RF*), defined as the ratio IC_{50} in A2780cisR/IC_{50} in A2780 cells. [c] Modulation Factor (*MF*), defined as the ratio IC_{50} in A2780cisR/IC_{50} in A2780cisR+BSO.

Cytotoxic activity

To analyze the potential of complexes **6**, **8**, **10** and **12** as anti-tumour agents, the cytotoxic activity towards the human epithelial ovarian carcinoma cells sensitive (A2780) and resistant (A2780cisR) to cisplatin was tested. For comparison purposes the cytotoxicity of cisplatin was evaluated under the same experimental conditions. The ovarian cancer cell lines were exposed to increasing concentrations of the different Pt complexes for 72 h. After this time, the cellular viability was determined by the colorimetric MTT assay (MTT = 3-(4,5-dimethylthiazol-2-yl)-2,5-diphenyltetrazolium bromide). The viability of cells in the presence of the tested compounds was compared to that observed in control cultures and the inhibition of growth (%) was calculated. The IC_{50} (*i.e.*, the concentration producing 50% inhibition of growth) was determined and expressed in μM concentration (Table 3).

Cisplatin-like complexes 6 and 8

Table 3 shows that in A2780 cells and for the drug treatment period of 72 h, complex **6** displayed the lower IC_{50} value. It is known that the substitution on nitrogen coordinating atoms (the pz*N ring in this case) is detrimental for the cytotoxic activity of diamine Pt(II) complexes.[33] However, the lipophilicity of **6** could compensate for this feature. In fact, complex **6** is more lipophilic than cisplatin and its cellular uptake is higher than that of cisplatin (see below), in agreement with the exponential correlation between log$P_{o/w}$ and uptake.[28]

Complex **8**, the methylated analogue of **6**, is less cytotoxic. In fact, the steric hindrance of additional methyl groups on nitrogen coordinating atoms causes higher values for IC_{50}.[34] On the contrary, the methylation on carbon atoms of a ethylenediamine ligand is far less detrimental since it has a lesser negative impact on the interaction with DNA. In the case of **8**, the methylation is on the pz*N ring and not directly on nitrogens; however, this methylation increases the bulkiness of the complex on one side. This could hinder the interaction with DNA. This hindrance makes complex **8** similar to an intermediate situation in the possible combination of N-methylation in a series of ethylenediamine substituted at different positions.[34] Although complex **8** was about 10 times less active than cisplatin, it greatly retained its activity in the A2780cisR cell line and presented a lower resistance factor (defined as IC_{50} in A2780cisR/IC_{50} in A2780) compared to cisplatin (1.3 *vs.* 5.6)

Cationic complexes 10 and 12

Most of the triamine-Pt(II) compounds, able to bind DNA in a monofunctional way, have very low cytotoxicity, including [PtCl(dien)]Cl.[35] On the contrary, some *cis*-[Pt(Am)Cl(NH_3)$_2$]Cl cations, in which Am is a derivative of pyridine, pyrimidine, purine, or aniline, inhibit DNA synthesis, specifically block DNA polymerases at platinated guanosine residues and are active against *in vivo* tumor models.[36]

In particular, transcription is strongly inhibited by *cis*-[PtCl(NH_3)$_2$(py)]$^+$ (cDPCP, py = pyridine) whereas adducts of other monofunctional platinum compounds like [PtCl(dien)]Cl, which would not cause the same steric hindrance, are much less effective. Although cDPCP blocks transcription nearly as efficiently as cisplatin, repair of cDPCP adducts by the nucleotide excision repair apparatus is reduced relatively to cisplatin. Therefore, cDPCP adducts should persist longer than those of cisplatin.[37]

Therefore, the activity of triamine complexes seems to be related to their steric hindrance. In fact, dien represents the simplest model of ligands **3** and **4** and its corresponding Pt complex, [PtCl(dien)]Cl, showed in our hands an IC_{50} value >300 μM with both A2780 and A2780cisR cell lines. Complex **10**, bulkier than [PtCl(dien)]Cl, shows higher activity and its methylated analogue **12** has a further improved cytotoxicity.

All biological experiments were performed also by using DMF as co-solvent (to a final 0.5% content). This solvent is quite toxic to cells (the cell viability in the controls never exceeded 75%), but it has been used here to study the influence of the formation of Pt-DMSO species on the citotoxicity. The IC_{50} values and the general trends were the same, within experimental error. This finding points out that the formation of solvated Pt-DMSO species is not detrimental of the final potency.

Effect of glutathione levels on cytotoxicity

Depletion of intracellular glutathione (GSH) has been shown *in vitro* to reverse resistance to a variety of anticancer drugs.[38] The effect of depletion of GSH levels by buthionine-*S*,*R*-sulfoximine (BSO), a selective inhibitor of glutathione synthase, was investigated in the A2780cisR cell line which contains elevated levels of GSH.[39] Results showed that when GSH levels in A2780cisR are depleted by preincubation with BSO, the resistance of the A2780cisR cell line decreases for all compounds (Table 3), although in a more pronounced way for cisplatin. The influence of lowering the GSH levels on the cytotoxicity, may be quantified by the modulation factor (*MF*), defined as the ratio IC_{50} in A2780cisR/IC_{50} in A2780cisR+BSO. For compounds **6**, **8**, **10** and **12**, the measured MF factors spanned between 1.5 and 2.9, while cisplatin has shown a value of 4.5. These results show that the Pt(II) complexes anchored by the pyrazolyl-containing chelators are less prone to undergo deactivation by glutathione, which seems to indicate that they might be less reactive against GSH compared to cisplatin. It is worth noting that picoplatin, a new generation platinum, overcomes platinum resistance because of the presence of the bulky picoline ligand; picoplatin has been shown to be less conjugated to GSH and methionine.[40]

Table 4 Total cellular platinum levels found in the cell lines A2780 ovarian carcinoma and its cisplatin-resistant variant A2780cisR after 24 h continuous treatment with compounds **6**, **8**, **10** and **12** and the reference complex cisplatin at 10 μM final concentration

	Total cellular platinum levels (pmole Pt 10^{-6} cells)	
Complex	A2780	A2780cisR
6	46.9 ± 1.3	81.3 ± 2.4
8	40.3 ± 0.5	47.5 ± 0.3
10	21.6 ± 1.7	42.5 ± 0.3
12	37.5 ± 1.6	76.4 ± 0.4
Cisplatin	37.6 ± 0.4	37.1 ± 0.1

Results are mean ± SD of measurements obtained from two independent experiments each one with six replicates.

Platinum uptake studies

ICP-MS technique was chosen to perform Pt uptake studies. Table 4 gives the total cellular Pt levels (expressed as picomoles Pt 10^{-6} cells) found in the ovarian carcinoma cells A2780 and A2780cisR after 24 h continuous treatment with the complexes at 10 μM final concentration.

The total cellular Pt levels showed by **6**, **8**, **10**, and **12** on A2780 cells span from 21.6 to 46.9 pmol Pt 10^{-6} cells, and cisplatin falls into this range. On the contrary, on A2780cisR the range of total cellular Pt levels increases to 42.5–81.3 pmol Pt 10^{-6} cells, while the value of cisplatin remains almost the same. Interestingly, these data point out that the complexes under investigation were accumulated more efficiently in the cisplatin-resistant cell line. In particular, for complex **8** a 1.2 factor is observed, while the total cellular Pt levels for **6**, **10**, and **12** are twice as high in A2780cisR. For the last three complexes, the uptake values are in tune with the measured log k'. On the contrary, in the case of cisplatin and complex **8**, the uptake values do not fit with lipophilicity. This result shows that cellular uptake *per se* may not reflect the antitumour activity of the complexes. In fact, the antiproliferative effect depends on the persistence of the reactive metabolites in the cells, which is the result of the equilibrium between influx and efflux.[41] This equilibrium is affected by several factors, including decreased Pt uptake by tumour cells and increased cellular detoxification due to GSH and metallothioneins (MTs). The strong reactivity of platinum compounds with S-donor molecules leads to the formation of very stable intracellular thiol-modified Pt(II) drugs that are exported from the cell by GS-X efflux pumps.[42] The uptake

values for cisplatin and **8** may be related to the role of GSH and MTs in their detoxification. This hypothesis is corroborated by the highest MF values in the series of complexes studied. Albeit the pyrazolyl-Pt(II) complexes are in general less prone to undergo deactivation (Table 3), surprisingly compound **8** seems to be more reactive towards GSH.

DNA Interaction

DNA damage induced by cisplatin and complexes **6**, **8, 10** and **12** was studied *in vitro* by monitoring the drug-induced conformational change of supercoiled ϕX174 plasmid DNA. Closed circular, rather than linear, DNA was used since this assay has been shown to be a sensitive monitor of small tertiary structural changes in the double helix produced both by intercalators and by covalent binding platinum complexes.[43] Moreover, the superhelical nature better mimics that of certain forms of intracellular DNA, such as chromatin.[44] Closed circular, supercoiled DNA was treated at 37 °C for a 24 h incubation period in phosphate buffer (pH 7.2) with various concentrations of cisplatin or Pt(II) complexes. The dose-dependent conformational changes of the treated DNA were detected by agarose gel electrophoresis.

As shown in Fig. 4, the electrophoretic mobilities of both the nicked and closed circular DNAs change. After 24 h of incubation, all the Pt(II) complexes were able to induce conformational changes in DNA, following the same pattern of cisplatin, but differing in the extent of the effect.

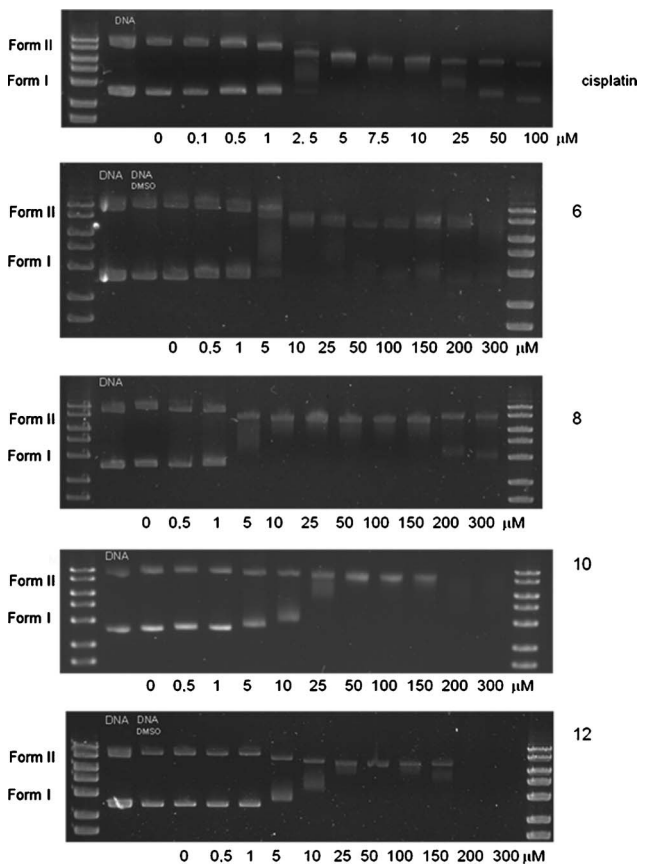

Fig. 4 Interaction between supercoiled ϕX174 plasmid DNA and cisplatin and complexes **6**, **8**, **10** and **12**, after 24 h of incubation at 37 °C in phosphate buffer (pH 7.2). Forms I and II are supercoiled and nicked circular forms of DNA, respectively.

The mobility of the nicked DNA band (form II) increases with increased platinum binding. This indicates the shortening of the DNA helix, as the platinum complexes will produce a more compact DNA structure on binding.

Even more substantial are the changes in the electrophoretic mobility of the supercoiled DNA with platinum binding. The electrophoresis mobility of the supercoiled DNA diminishes with increasing concentrations of complexes, until a minimum, where the nicked and supercoiled DNAs co-migrate in the electrophoresis gel (the coalescence point). Further increase in concentrations causes increased mobility of the supercoiled form. The coalescence point is detected at a concentration of 5 μM for cisplatin, between 5 and 10 μM for complexes **6** and **8**, and between 25 and 50 μM for complexes **10** and **12**. These changes are caused by the Pt(II) complexes, that unwind and rewind supercoiled DNA by binding covalently to the bases in a manner similar to that observed for cisplatin. It has been proposed that platination disrupts the hydrogen bond formation and causes localized unwinding of the duplex DNA. The interruption of base pairing produces single-stranded regions that, under the conditions of low ionic strength in the gels, collapse and reduce the effective length of the DNAs.[43,44] This has been confirmed by electron microscopy, that revealed a pronounced and progressive shortening of the DNA with increased platinum binding.[44]

Noteworthy, the diminished mobility of the supercoiled DNA was not observed when DNA was electrophoresed in the presence of ethidium bromide at 0.5 μg mL^{-1}. This is consistent with previous observations that showed that addition of ethidium bromide to the incubation mixture during platination of DNAs diminishes the shortening effect.[44]

We can conclude that complexes **6** and **8**, similarly to cisplatin, accelerated the mobility of the relaxed form of DNA, indicating the formation of bifunctional adducts. The smaller unwinding of the supercoiled form induced by the cationic complexes **10** and **12** is compatible with monofunctional adducts.

Experimental

All chemicals (analytical grade) were obtained from Aldrich, except K_2PtCl_4 from Johnson Matthey, and used as received. Complex *cis*-[$Pt(DMSO)_2Cl_2$] was prepared according to the method of Kukushkin *et al.*[45] The bidentate pz*N ligands (**1** and **2**)[13] and the tridentate pz*NN ligands (**3** and **4**)[14] were synthesized according to literature procedures.

Purity of compounds was assessed by analytical RP-HPLC (see below), elemental analysis (C, H, N) and determination of Pt content by inductively coupled plasma-optical emission spectroscopy (ICP-OES). Elemental analyses were carried out with a EA3000 CHN Elemental Analyzer (EuroVector, Milano, Italy). Platinum was quantified by means of a Spectro Genesis ICP-OES spectrometer (Spectro Analytical Instruments, Kleve, Germany) equipped with a crossflow nebulizer. In order to quantify the platinum concentration the Pt 299.797 line was selected. A platinum standard stock solution of 1000 mg L^{-1} was diluted in 1.0% v/v nitric acid to prepare calibration standards. The elemental analyses and Pt content were within ±0.4% absolute of the theoretical value.

The multinuclear NMR spectra were measured on a JEOL Eclipse Plus operating at 400 MHz (^{1}H), 100.5 MHz (^{13}C) and 85.9 MHz (^{195}Pt with a spectral window of 2000 ppm), respectively. ^{1}H and ^{13}C NMR chemical shifts were reported in parts per million (ppm) referenced to solvent resonances; for D_2O measurements 1% methanol was added as ^{13}C internal reference. See Fig. 1 for the numbering scheme. ^{195}Pt NMR spectra were recorded using a solution of K_2PtCl_4 in saturated aqueous KCl as the external reference. The shift for K_2PtCl_4 was adjusted to −1628 ppm from Na_2PtCl_6 ($\delta = 0$ ppm).

Electrospray mass spectra (ESI-MS) were obtained using a Micromass ZMD mass spectrometer (Micromass, Manchester, UK). Typically, a diluted solution of the compound in methanol (with 1–2% of the suitable co-solvent) was delivered directly to the spectrometer source at 0.01 mL min^{-1}, using a Hamilton microsyringe controlled by a single-syringe infusion pump. The nebulizer tip operated at 3000–3500 V and 150 °C, with nitrogen used both as a drying and a nebulizing gas. The cone voltage was usually 30 V. $[M–X+DMSO]^+$ for **5–8** and $[M–X]^+$ (X = I, Cl) for **9–12** peaks were assigned on the basis of the *m/z* values and of the simulated isotope distribution patterns.

Ion chromatography, used to evaluate the exchange of the counter ions, was performed by means of a Dionex DX500 ion chromatograph (Dionex Corp., Sunnyvale, CA, USA) equipped with a Dionex GP40 Gradient Pump and a Dionex ED40 Electrochemical Detector. An anion-exchange Dionex IonPac AS14A (4 × 250mm) column with a AG14A pre-column was used as stationary phase, while a 8 mM carbonate/1 mM bicarbonate buffer was used as eluent (flow = 1 mL min^{-1}; 100 mM H_2SO_4 was used as chemical suppressor).

Synthesis of Pt-complexes containing bidentate pz*N ligands, 5–8

$K_2[PtCl_4]$ (1.00 g, 2.41 mmol) was dissolved in water (30 mL) and KI (2.40 g, 14.5 mmol) was added in the dark to the mixture. After about 30 min it was filtered to remove some solid impurities. The oily ligand pz*N (**1** or **2**, 2.17 mmol) was added dropwise to the filtrate. Fine yellow–brown crystals of *cis*-$[Pt(pz*N)I_2]$ almost immediately precipitated. After 15 min the compound was separated by centrifugation and washed with cold water, ethanol and diethyl ether and dried under vacuum (80–90% yield). *cis*-$[Pt(pz*N)I_2]$ (1.87 mmol) was then suspended in an aqueous solution (100 mL) of Ag_2SO_4 (570 mg, 1.83 mmol) and the mixture was stirred for 20 h in the dark; after that the silver iodide precipitate was removed by filtration. KCl (2.92 g, 39.2 mmol) was then added to the filtrate. The mixture was stirred for 20 h and then centrifuged to separate the precipitated *cis*-$[Pt(pz*N)Cl_2]$ product. The solid obtained was washed several times with water, ethanol and diethyl ether and dried under vacuum (50–60% yield).

5. ^{1}H NMR (400 MHz; DMF-d_7): δ 8.523 (1H, d, ^3J = 2.56 Hz, 5-H or 3-H), 8.130 (1H, d, ^3J = 2.56 Hz, 5-H or 3-H), 6.512 (1H, t, ^3J = 2.56 Hz, 4-H), 5.504 (2H, m, NH_2), 4.631 (2H, m, 2-H), 2.954 (2H, m, 1-H) ppm; ^{13}C NMR (100.5 MHz; DMF-d_7): δ 144.298 (C5), 133.906 (C3), 106.171 (C4), 52.039 (C2), 41.846 (C1) ppm; ^{195}Pt NMR (85.9 MHz; DMF-d_7): δ −3365 ppm. ESI-MS (methanol:DMSO = 99 : 1): 510.02 (89.95), 511.00 (100.00), 512.02 (82.99), 513.03 (11.95), 513.99 (40.47) *m/z*, calcd for $C_7H_{15}IN_3OPtS$ 509.96 (88.85), 510.96 (100.00), 511.96 (81.81), 512.96 (11.80), 513.96 (23.32) $[M–I+DMSO]^+$.

6. ^{1}H NMR (400 MHz; DMF-d_7): δ 8.232 (1H, d, ^3J = 2.56 Hz, 5-H or 3-H), 8.120 (1H, d, ^3J = 2.56 Hz, 5-H or 3-H), 6.488 (1H, t, ^3J = 2.56 Hz, 4-H), 5.627 (2H, m, NH_2), 4.530 (2H, m, 2-H), 2.957 (2H, m, 1-H) ppm; ^{13}C NMR (100.5 MHz; DMF-d_7): δ 140.888 (C5), 134.036 (C3), 105.812 (C4), 51.702 (C2), 41.746 (C1) ppm; ^{195}Pt NMR (85.9 MHz; DMF-d_7): δ −2261 ppm. ESI-MS (methanol:DMSO = 99 : 1): 418.14 (82.62), 419.19 (90.22), 420.14 (100.00), 421.33 (40.49), 422.24 (44.05), 423.17 (6.04), 424.10 (7.37) *m/z*, calcd for $C_7H_{15}ClN_3OPtS^+$ 418.02 (81.20), 419.03 (90.79), 420.03 (100.00), 421.02 (39.72), 422.03 (44.91), 423.03 (5.49), 424.03 (7.69) $[M–Cl+DMSO]^+$.

7. ^{1}H NMR (400 MHz; DMF-d_7): δ 6.149 (1H, s, 4-H), 5.429 (2H, m, NH_2), 4.696 (2H, m, 2-H), 2.958 (2H, m, 1-H), 2.526 (3H, s, CH_3), 2.438 (3H, s, CH_3) ppm; ^{13}C NMR (100.5 MHz; DMF-d_7): δ 150.882 (C5), 142.318 (C3), 107.326 (C4), 49.202 (C2), 41.868 (C1), 16.817 (CH_3) and 10.967 (CH_3) ppm; ^{195}Pt NMR (85.9 MHz; DMF-d_7): δ −3357 ppm. ESI-MS (methanol:DMSO = 99 : 1): 538.03 (86.08), 538.98 (100.00), 540.01 (82.45), 541.13 (13.18), 542.03 (23.96) *m/z*, calcd for $C_9H_{19}IN_3OPtS^+$ 537.99 (87.10), 538.99 (100.00), 539.99 (82.44), 540.99 (13.41), 542.00 (23.14) $[M–I+DMSO]^+$.

8. ^{1}H NMR (400 MHz; DMF-d_7): δ 6.107 (1H, s, 4-H), 5.554 (2H, m, NH_2), 4.549 (2H, m, 2-H), 2.843 (2H, m, 1-H), 2.519 (3H, s, CH_3) and 2.414 (3H, s, CH_3) ppm; ^{13}C NMR (100.5 MHz; DMF-d_7): δ 151.716 (C5), 142.180 (C3), 107.242 (C4), 49.668 (C2), 42.021 (C1), 14.087 (CH_3) and 10.922 (CH_3) ppm; ^{195}Pt NMR (85.9 MHz; DMF-d_7): δ −2213 ppm. ESI-MS (methanol:DMSO = 99 : 1): 446.21 (78.21), 447.21 (89.47), 448.21 (100.00), 449.21 (41.22), 450.21 (44.38), 451.24 (6.37), 452.242 (7.00) *m/z*, calcd for $C_9H_{19}ClN_3OPtS^+$ 446.06 (79.59), 447.06 (90.77), 448.06 (100.00), 449.06 (41.16), 450.06 (44.90), 451.06 (6.39), 452.06 (7.67) $[M–Cl+DMSO]^+$.

Synthesis of Pt-complexes containing tridentate pz*NN ligands, 9–12

Method I (Dhara),[17] Synthesis of iodido complexes 9 and 11. $K_2[PtCl_4]$ (0.415 g, 1 mmol) was dissolved in water (10 mL) and treated with a solution of KI (1.660 g, 10 mmol) in the same solvent (5 mL). The solution was stirred for 10 min in the dark at room temperature and then treated with a stoichiometric amount of pz*NN (**3** or **4**, 1 mmol) in DMF (3 mL). After 24 h the yellow precipitate of [Pt(pz*NN)I]I was separated by centrifugation, washed with water and dried under vacuum. The complex was dissolved in a small quantity of DMF and then precipitate with water, and again washed with water and dried under vacuum. Yield: 50–60%.

9. ^{1}H NMR (400 MHz; DMF-d7): δ 8.49 (1H, d, *J* = 2.56 Hz, 5-H or 7-H), 8.29 (1H, d, *J* = 2.56 Hz, 5-H or 7-H), 7.30 (1H, m, NH), 6.52 (1H, t, *J* = 2.56 Hz, H-6), 6.05 (2H, m, NH_2), 5.00 (1H, m, 4-H), 4.61 (1H, m, 4-H′), 3.58–3.46 (2H, m, 3-H), 3.07–2.98 (2H, m, 2-H), 2.82–2.70 (2H, m, 1-H), ppm; ^{13}C NMR (100.5 MHz; DMF-d7): δ 146.73 (C7 or C5), 135.13 (C7 or C5), 107.27 (C6), 57.23 (C2), 52.19 (C3), 50.02 (C4 or C1), 47.70(C4 or C1) ppm; ^{195}Pt NMR (85.9 MHz; DMF-d7): δ −3079 ppm. ESI-MS (methanol:acetone = 98 : 2): 475.09 (85.09), 476.12 (100.00), 477.13 (77.29), 478.09 (6.62), 479.03 (20.28) *m/z*, calcd for $C_7H_{14}IN_4Pt^+$474.99 (89.14), 475.99 (100.00), 476.99 (77.56), 477.99 (6.86), 478.99 (19.79) $[M–I]^+$.

11. ^{1}H NMR (400 MHz; DMF-d7): δ 7.20 (1H, m, NH), 6.19 (1H, s, H-6), 5.80 (2H, m, NH_2), 4.94 (1H, m, 4-H), 4.58 (1H, m, 4-H′), 3.41–3.25 (2H, m, 3-H), 3.08–3.01 (2H, m, 2-H), 2.90–2.80 (2H, m, 1-H), 2.48 (3H, s, CH_3), 2.46 (3H, s, CH_3) ppm; ^{13}C NMR (100.5 MHz; DMF-d7): δ 152.15 (C7 or C5), 143.42 (C7 or C5), 107.59 (C6), 57.58 (C2), 50.68 (C3), 49.26 (C4 or C1), 49.19 (C1 or C4), 16.85 (CH_3), 11.15 (CH_3) ppm; ^{195}Pt NMR (85.9 MHz; DMF-d7): δ –3115 ppm. ESI-MS (methanol:acetone = 98 : 2): 503.47 (87.30), 504.43 (100.00), 505.46 (78.31), 506.22 (8.45), 507.30 (19.52) *m*/*z*, calcd for $C_9H_{18}IN_4Pt^+$ 503.02 (87.35), 504.02 (100.00), 505.02 (78.28), 506.03 (8.48), 507.03 (19.56) $[M–I^-]^+$.

Method I (Dhara),[17] Synthesis of chlorido complexes 10 and 12. To a solution of $AgNO_3$ (0.140 g; 0.827 mmol) in 10 mL water, [Pt(pz*NN)I]I (0.276 mmol) in 10 mL water was added and the mixture was stirred in the dark for 4 h at 50° C. Then KCl (0.092 g; 1.24 mmol) was added and the solution was stirred at room temperature for 18 h. After stirring, the mixture was centrifuged to remove AgI and AgCl. The filtrate was evaporated under reduced pressure to reduce the volume and then cooled at 4 °C to favor the precipitation of the yellow–pink product $[Pt(pz*NN)Cl]NO_3$.

$[Pt(pz*NN)Cl]NO_3$ was dissolved in water and added to a suspension of anion exchange resin (Amberlite® IRA-400, Rohm & Haas Co. in chloride form) in water (20 mL). After 30 min. the suspension was filtered and the filtrate was dried under reduced pressure and dissolved in ethanol, to remove excess KCl. Ethanol was dried under reduced pressure to get the white product [Pt(pz*NN)Cl]Cl. Yield: 30–40% (from the iodido complex).

10. ^{1}H NMR (400 MHz; CD_3OD): δ 8.29 (1H, d, J = 2.56 Hz, 5-H or 7-H), 7.95 (1H, d, J = 2.56 Hz, 5-H or 7-H), 6.95 (1H, m, NH), 6.45 (1H, t, J = 2.56 Hz, 6-H), 5.85 (2H, m, NH_2), 4.80–4.75 (1H, m, 4-H), 4.32–4.25 (1H, m, 4-H′), 3.49–3.27 (2H, m, 3-H), 3.00–2.76 (4H, m, 2-H), 2.70–2.59 (2H, m, 1-H) ppm; ^{13}C NMR (100.5 MHz; CD_3OD): δ 142.71 (C5 or C7), 135.87 (C5 or C7), 107.62 (C6), 59.19 (C2), 52.55 (C3), 51.58 (C4), 46.55 (C1) ppm; ^{195}Pt NMR (85.9 MHz; CD_3OD): δ –2691 ppm. ESI-MS (methanol:water = 98 : 2): 383.18 (83.74), 384.18 (94.40), 385.18 (100.00), 386.14 (38.36), 387.18 (40.15), 388,22 (4.19), 388,98 (7.06) *m*/*z*, calcd for $C_7H_{14}ClN_4Pt^+$ 383.05 (84.67), 384.06 (94.33), 385.05 (100.00), 386.05 (36.62), 387.06 (42.04), 388.06 (3.82), 389.06 (6.04) $[M–Cl]^+$.

12. ^{1}H NMR (400 MHz; CD_3OD): δ 6.88 (1H, m, NH), 6.06 (1H, s, 6-H), 5.63 (2H, m, NH_2), 4.80–4.75 (1H, m, 4-H), 4.33 (1H, m, H-4′), 3.05–2.80 (4H, m, H-2 and H-3), 2.75–2.55 (2H, m, H-1), 2.46 (3H, s, CH_3), 2.38 (3H, s, CH_3) ppm; ^{13}C NMR (100.5 MHz; CD_3OD): δ 153.65 (C5 or C7), 144.01 (C5 or C7), 108.52 (C6), 59.65 (C2), 51.72 (C3), 49.84 (C4), 47.58 (C1), 14.22 (CH_3), 11.47 (CH_3) ppm; ^{195}Pt NMR (85.9 MHz; CD_3OD): δ –2657 ppm. ESI-MS (methanol:water = 98 : 2): 411.14 (82.92), 412.21 (94.20), 413.26 (100.00), 414.09 (38.09), 415.09 (41.95), 416.19 (4.68), 417.08 (6.14) *m*/*z*, calcd for $C_9H_{18}ClN_4Pt^+$ 411.09 (82.90), 412.09 (94.25), 413.09 (100.00), 414.09 (38.09), 415.09 (41.99), 416.09 (4.68), 417.09 (6.01) $[M–Cl]^+$.

Method II (Annibale *et al.*). [18] A solution of pz*NN (**3** or **4**, 0.71 mmol) in methanol (10 mL) was added with stirring to a suspension of *cis*-$[Pt(DMSO)_2Cl_2]$ (0.30 g, 0.71 mmol) in methanol (50 mL), and the mixture was refluxed for 1 h. The resulting clear yellow solution was cooled at room temperature and concentrated in a rotary evaporator. After removal of 5–10 mL a precipitate (above all unreacted *cis*-$[Pt(DMSO)_2Cl_2]$) formed and was removed with centrifugation. The volume was then reduced to *ca* 2 mL. Acetone was then added to precipitate the yellow–pink product that was washed several times with acetone and diethyl ether and dried in vacuo. The product [Pt(pz*NN)Cl]Cl was then dissolved in a small volume of water and acetone was added to precipitate the product that was washed and dried as described above. Yield: 60–70%.

X-ray analysis

Yellow crystals of **5** and **6**, and light pink-colourless crystals of **12** were obtained from slow diffusion of diethyl ether into an acetone, dimethylformamide or methanol solution of the complexes, respectively, at room temperature in a diethyl ether-saturated chamber for about 2 days. Suitable dimensional crystals were selected for X-ray single-crystal diffraction. The X-ray diffraction analysis of **5**, **6** and **12** was performed on a Bruker AXS APEX CCD area detector diffractometer, using graphite monochromated Mo-Kα radiation (0.71073 Å). Empirical absorption correction was carried out using SADABS.[46] Data collection and data reduction were done with the SMART and SAINT programs.[47] The structures were solved by direct methods with SIR97[48] and refined by full-matrix least-squares analysis with SHELXL-97[49] using the WINGX[50] suite of programmes. All non-hydrogen atoms were refined anisotropically. The remaining hydrogen atoms were placed in calculated positions. Molecular graphics were prepared using ORTEP3.[51] A summary of the crystal data, structure solution and refinement parameters are given in Table 5.†

Conductivity measurements

To assess the relative rate of solvolysis, complexes were dissolved in DMSO and diluted with Milli-Q water to a final 2% of organic solvent and 0.5 mM concentration of Pt compound. Conductivity measurements were performed with an Amel 160 conductimeter (Amel, Milan, Italy), at 37 °C and at various times (during 3 d).

Partition coefficient

Considering that RP-HPLC retention is due to partitioning between mobile and stationary phases, there is a correlation between partition coefficients and HPLC capacity factors ($k' = (t_R - t_0)/t_0$, where t_0 is the retention time for an unretained compound and t_R is the retention time of the analysed species). The chromatographic conditions were:[29,52] silica-based C18 gel as the stationary phase (5-μm Phenomenex Phenosphere NEXT C18 column 250 × 4.6 mm ID); flow rate = 0.75 mL min^{-1}; isocratic elution, UV–visible detector set at 210 nm; 10 mM NaCl was the internal reference to determine the column dead-time (t_0); a mobile phase containing 15 mM aqueous HCOOH/MeOH 80/20. Platinum complex solutions were 0.25 mM.

Cytotoxic activity

The human ovarian carcinoma cell lines (A2780 and A2780cisR) used in this study were grown in RPMI 1640 medium supplemented with 10% fetal bovine serum (FBS) and 2 mM L-glutamine in an atmosphere of 5% CO_2 at 37 °C.

Table 5 Crystallographic data for compounds **5**, **6** and **12**

	5	**6**	**12**
Formula	$C_5H_9I_2N_3Pt$	$C_5H_9Cl_2N_3Pt$	$C_9H_{18}Cl_2N_4Pt$
Mr	560.04	377.14	448.26
T/K	150(2) K	150(2) K	150(2) K
Crystal system	Orthorhombic	Orthorhombic	Monoclinic
Space group	$Pca2_1$	$Pca2_1$	*P21/n*
a/Å	17.8791(2)	16.7647(8)	11.9792(3)
b/Å	6.7986(6)	6.2596(3)	7.6707(2)
c/Å	8.3581(3)	8.2202(4)	15.2962(4)
α (°)	90	90	90
β (°)	90	90	102.4240(10)
γ (°)	90	90	90
V/Å^3	1015.95(10)	862.63(7)	1372.64(6)
Z	4	4	4
D_x/g cm^{-3}	3.661	2.904	2.169
μ/mm^{-1}	19.836	16.822	10.593
F(000)	976	688	848
Crystal size/mm	0.20 × 0.15 × 0.04	0.16 × 0.12 × 0.02	0.16 × 0.10 × 0.04
R(int)	0.0374	0.0383	0.0250
Number of reflections collected	4519	4918	6336
Number of unique reflections	2007	1551	2579
Goodness-of-fit on F^2	0.989	0.980	1.003
R_1	0.0269	0.0195	0.0197
wR_2 (all data)	0.0652	0.0424	0.0441

Cytotoxic activity was evaluated by the MTT assay (MTT = 3-(4,5-dimethylthiazol-2-yl)-2,5-diphenyltetrazolium bromide).[53] A2780 and A2780cisR cells were plated in 96-well sterile plates at a density of 8×10^3 cells per well with 200 µL of medium and were then incubated overnight. After attachment to the culture surface, cells were incubated with various concentrations of the complexes tested freshly dissolved in DMSO (except cisplatin that was solubilized in water) and diluted in the culture medium (DMSO final concentration < 1%) for 72 h at 37 °C. At the end of the incubation period, the compounds were removed and cells were incubated with 200 µL of MTT solution (0.5 mg mL^{-1}). After 3–4 h at 37 °C/5% CO_2, the medium was removed and the purple formazan crystals formed inside the cells were dissolved in 200 µL DMSO by thorough shaking. The cellular viability was evaluated by measurement of the absorbance at 570 nm by using a plate spectrophotometer (PowerWave Xs, Bio-Tek Instruments, Winooski, VT, USA). The cytotoxic effects of Pt complexes were quantitated by calculating the drug concentration inhibiting tumor cell growth by 50% (IC_{50}), based on non-linear regression analysis of dose–response data. For comparison, the cytotoxicity of cisplatin was evaluated under the same experimental conditions. All compounds were tested in at least two independent studies with six replicates.

In the GSH-depletion experiment, A2780cisR cells were pre-incubated for 2 h with 400 µM of buthionine-*S*,*R*-sulfoximine (BSO, Sigma) in medium. After incubation, medium with BSO was discarded and fresh solutions of the platinum complexes in medium (200 µL) were added to the cells and incubated in the presence of BSO in a final concentration of 25 µM. Control experiments were performed to evaluate the effect of BSO on cell viability. The growth inhibitory effect of Pt compounds after 72 h was then determined using the MTT assay.

Cellular Pt uptake

To measure the Pt uptake, *ca.* 10^6 cells/5 mL medium were treated with the complexes at 10 µM final concentration for 24 h, 37 °C. Then the cells were washed three times with ice-cold PBS solution, harvested and centrifuged following a method similar to that described by Gabano *et al.*[28,54] The cell suspension was dissolved with ultrapure HNO_3 (65%), obtained by subdestillation of nitric acid. The platinum content (^{195}Pt) was measured by a Thermo X-Series Quadrupole ICP-MS (Thermo Scientific), equipped with Ni cones and a glass concentric nebulizer (Meinhard, 1.0 mL min^{-1}) refrigerated with a Peltier system. The samples were diluted in ultrapure water, obtained from a MilliQ apparatus, in order to obtain 2.0% (v/v) nitric acid. Indium (^{115}In) at a concentration of 10 µM L^{-1} was used as internal standard. Standards were prepared from standard ICP-MS 71 C (Inorganic Venture) with a final concentration of 2.0% subboiled nitric acid and 10 µg L^{-1} of ^{115}In. The following quality control was applied: internal standard accepted variation between 80 and 120%; blank's concentrations inferior to the limit of detection (0.001 µg L^{-1}) and spikes recovery of added platinum between 89 and 105%.

DNA interaction

The plasmid DNA used for gel electrophoresis experiments was ϕX174 (Promega). DNA interaction was evaluated by monitoring the mobility of the supercoiled plasmid DNA (Sc – form I) and nicked circular DNA (Nck- form II). Each reaction mixture was prepared by adding 6 µL of water, 2 µL (200 ng) of supercoiled DNA, 2 µL of 100 mM stock Na_2HPO_4/HCl pH 7.2 buffer solution and 10 µL of the solution of the complex. The final reaction volume was 20 µL, the final buffer concentration was 10 mM and the final metal concentration varied from 0.1 and 0.5 to 100 and 300 µM (depending on the complex). Samples were typically incubated for 24 h at 37 °C, in the dark. After incubation, 5 µL of DNA loading buffer (0.25% bromophenol blue, 0.25% xylene cyanol, 30% glycerol in water, Applichem) were added to each tube and the sample was loaded onto a 0.8% agarose gel in TBE buffer (89 mM Tris–borate, 1 mM EDTA pH 8.3. Controls of non-incubated plasmid and of plasmid incubated with DMSO

were loaded on each gel electrophoresis. The electrophoresis was carried out for 2.5 h at 100 V. The gels were then stained with TBE buffer containing ethidium bromide (0.5 μg mL^{-1}). Bands were visualised under UV light and images captured using an AlphaImagerEP (Alpha Innotech). All samples in each figure were obtained from the same run.

Conclusions

A series of four Pt(II) complexes anchored by bidentate or tridentate pyrazolyl-alkylamine chelators bearing different substituents at the azolyl rings has been prepared and fully characterized. Their solution behavior has been evaluated (conductivity measurements and ESI-MS) together with lipophilicity measurements, cell uptake, antiproliferative properties, and DNA interaction. The dichlorido, neutral complexes, **6** and **8**, underwent hydrolysis/solvolysis to give mono-charged species (conductivity plateaued after 6–8 h), while the monochlorido cationic complexes, **10** and **12**, produced dicationic species (conductivity plateaued over a longer time, *i.e.* >17 h). The methylated compounds show a slower rate of hydrolysis, reflecting the highest steric environment of the complexes. The conductivity results, together with ESI-MS of the aged solutions, suggest a partial hydrolysis/solvolysis.

All complexes but **10** are less hydrophilic than cisplatin, in the order **10** < **12** < **6** < **8**, with the complexes with methylated ligands more lipophilic than non-methylated analogues. This trend is almost completely reflected in the total cellular Pt levels on A2780 cell lines. Interestingly, while the Pt uptake for cisplatin on both A2780 and A2780cisR cell lines is very similar, the complexes under investigation were found to be accumulated more efficiently in the cisplatin-resistant cells.

Albeit all the complexes were less active than cisplatin on ovarian carcinoma A2780 cell line, greatly retained their activity in the cisplatin-resistant A2780cisR cell line and presented a lower resistance factor compared to cisplatin. The Pt(II) complexes under investigation were less prone to undergo deactivation by glutathione, believed to be the major cellular target of cisplatin that inactivates the drug by binding to it irreversibly.

Finally, the DNA interaction studies showed that dichlorido complexes **6** and **8**, similarly to cisplatin, induce the formation of bifunctional adducts, while the behaviour of monochlorido complexes **10** and **12** is compatible with monofunctional adducts.

Acknowledgements

C. S. F. and S. G. wish to thank the Fundação para a Ciência e Tecnologia (FCT) for a research grant and a Postdoctoral research grant (SFRH/BPD/29564/2006), respectively. The authors would like to acknowledge the COST Action D39 (for a STSM to C. S. F.), as well as FEDER and FCT for financial support (PTDC/QUI/66813/2006). The research was carried out within the framework of the European Cooperation COST Action D39 (Metallo-Drug Design and Action) and Consorzio Interuniversitario di Ricerca in Chimica dei Metalli nei Sistemi Biologici (CIRCMSB, Bari, Italy). The authors thank Dr Eugénio Soares of LCA-Aveiro University for the ICP-MS platinum uptake studies.

Notes and references

1 N. J. Wheate, S. Walker, G. E. Craig and R. Oun, *Dalton Trans.*, 2010, **39**, 8113–8127.
2 L. R. Kelland, *Nat. Rev. Cancer*, 2007, **7**, 573–584.
3 P. J. Dyson and G. Sava, *Dalton Trans.*, 2006, 1929–1933.
4 T. Nakamura and T. Miki, *Int. J. Urol.*, 2010, **17**, 148–157.
5 B. T. Hennessy, R. L. Coleman and M. Markman, *Lancet*, 2009, **374**, 1371–1382.
6 F. Basolo, F. J. Chatt, H. B. Gray, R. G. Pearson and B. L. Shaw, *J. Chem. Soc.*, 1961, 2207–2215.
7 (*a*) Y. Chen, Z. Guo, S. Parsons and P. J. Sadler, *Chem.–Eur. J.*, 1998, **4**, 672–676; (*b*) J. F. Holford, F. I. Raynaud, B. A. Murrer, K. Grimaldi, J. A. Hartley, M. J. Abrams and L. R. Kelland, *Anti–Cancer Drug Des.*, 1998, **13**, 1–18; (*c*) F. I. Raynaud, F. E. Boxall, P. M. Goddard, M. Valenti, M. Jones, B. A. Murrer, M. Abrams and L. R. Kelland, *Clin. Cancer Res.*, 1997, **3**, 2063–2074.
8 J. R. Eckardt, D. L. Bentsion, O. N. Lipatov, I. S. Polyakov, F. R. MacKintosh, D. A. Karlin, G. S. Baker and H. Breitz, *J. Clin. Oncol.*, 2009, **27**, 2046–2051.
9 (*a*) S. Komeda, M. Lutz, L. A. Spek, Y. Yamanaka, T. Sato, S. Chikuma and J. Reedijk, *J. Am. Chem. Soc.*, 2002, **124**, 4738–4746; (*b*) C. Chopard, C. Lenoir, S. Rizzato, M. Vidal, J. Arpalahti, L. Gabison, A. Albinati, C. Garbay and J. Kozelka, *Inorg. Chem.*, 2008, **47**, 9701–9705.
10 J. D. Correia, A. Paulo and I. Santos, *Curr. Radiopharm.*, 2009, **2**, 277–294.
11 R. F. Vitor, M. Videira, F. Marques, A. Paulo, J. C. Pessoa, G. Viola, G. G. Martins and I. Santos, *ChemBioChem*, 2008, **9**, 131–142.
12 (*a*) R. F. Vitor, T. Esteves, F. Marques, P. Raposinho, A. Paulo, S. Rodrigues, J. Rueff, S. Casimiro, L. Costa and I. Santos, *Cancer Biother. Radiopharm.*, 2009, **24**, 551–563; (*b*) T. Esteves, C. Xavier, S. Gama, F. Mendes, P. D. Raposinho, F. Marques, A. Paulo, J. Costa Pessoa, J. Rino, G. Viola and I. Santos, *Org. Biomol. Chem.*, 2010, **8**, 4104–4116.
13 C. Moura, R. F. Vítor, L. Maria, A. Paulo, I. C. Santos and I. Santos, *Dalton Trans.*, 2006, 5630–5640.
14 (*a*) S. Alves, J. D. G. Correia, A. Paulo, L. Gano, J. Smith and I. Santos, *Bioconjugate Chem.*, 2005, **16**, 438–449; (*b*) S. Alves, A. Paulo, J. D. G. Correia, A. Domingos and I. Santos, *J. Chem. Soc., Dalton Trans.*, 2002, 4714–4719.
15 S. C. Dhara, *Indian J. Chem.*, 1970, **8**, 193–194.
16 (*a*) R. C. Harrison and C. A. McAuliffe, *Inorg. Chim. Acta*, 1980, **46**, L15–L16; (*b*) F. D. Rochon and L. M. Gruia, *Inorg. Chim. Acta*, 2000, **306**, 193–204.
17 (*a*) N. G. Di Masi, F. P. Intini, C. Pacifico, L. Maresca and G. Natile, *Inorg. Chim. Acta*, 2000, **310**, 27–30; (*b*) G. W. Watt and W. A. Cude, *Inorg. Chem.*, 1968, **7**, 335–338.
18 G. Annibale, M. Brandolisio and B. Pitteri, *Polyhedron*, 1995, **14**, 451–453.
19 (*a*) J. Pons, G. Aragay, J. García–Antón, T. Calvet, M. Font–Bardia and J. Ros, *Inorg. Chim. Acta*, 2010, **363**, 911–917; (*b*) G. Aragay, J. Pons, V. Branchadell, J. García–Antón, X. Solans, M. Font–Bardia and J. Ros, *Aust. J. Chem.*, 2010, **63**, 257–269; (*c*) M. C. Castellano, J. Pons, J. García–Antón, X. Solans, M. Font–Bardia and J. Ros, *Inorg. Chim. Acta*, 2008, **361**, 2491–2498.
20 B. M. Still, P. G. Anil Kumar, J. R. Aldrich–Wright and W. S. Price, *Chem. Soc. Rev.*, 2007, **36**, 665–686.
21 (*a*) M. S. Ali and A. R. Khokhar, *J. Inorg. Biochem.*, 2003, **96**, 452–456; (*b*) M. S. Ali, S. R. Ali Khan, H. Ojima, I. Y. Guzman, K. H. Whitmire, Z. H. Siddik and A. R. Khokhar, *J. Inorg. Biochem.*, 2005, **99**, 795–804.
22 T. M. Gilbert and T. Ziegler, *J. Phys. Chem. A*, 1999, **103**, 7535–7543.
23 (*a*) E. Pantoja, A. Gallipoli, S. van Zutphen, S. Komeda, D. Reddy, D. Jaganyi, M. Lutz, D. M. Tooke, A. L. Spek, C. Navarro–Ranninger and J. Reedijk, *J. Inorg. Biochem.*, 2006, **100**, 1955–1964; (*b*) M. Guerrero, J. Pons, T. Parella, M. Font–Bardia, T. Calvet and J. Ros, *Inorg. Chem.*, 2009, **48**, 8736–8750.
24 (*a*) F. D. Rochon and V. Buculei, *Inorg. Chim. Acta*, 2004, **357**, 2218–2230; (*b*) C. Tessier and F. D. Rochon, *Inorg. Chim. Acta*, 2010, **363**, 2652–2660; (*c*) S. W. A. Bligh, A. Bashall, C. Garrud, M. McPartlin, N. Wardle, K. White, S. Padhye, V. Barve and G. Kundu, *Dalton Trans.*, 2003, 184–188.
25 S. J. Berners–Price and T. G. Appleton, in *Platinum–based Drugs in Cancer Therapy*, ed. L. R. Kelland and N. P. Farrell, Humana Press, Totowa NJ, 2000, pp. 3–35.

26 S. J. S. Kerrison and P. J. Sadler, *J. Chem. Soc., Chem. Commun.*, 1977, 861–863.
27 (*a*) A. J. Di Pasqua, J. Goodisman, D. J. Kerwood, B. B. Toms, R. L. Dubowy and J. C. Dabrowiak, *Chem. Res. Toxicol.*, 2006, **19**, 139–149; (*b*) S. Bombard, M. B. Gariboldi, E. Monti, E. Gabano, L. Gaviglio, M. Ravera and D. Osella, *JBIC, J. Biol. Inorg. Chem.*, 2010, **15**, 841–850.
28 (*a*) A. R. Ghezzi, M. Aceto, C. Cassino, E. Gabano and D. Osella, *J. Inorg. Biochem.*, 2004, **98**, 73–78; (*b*) J. A. Platts, D. E. Hibbs, T. W. Hambley and M. D. Hall, *J. Med. Chem.*, 2001, **44**, 472–474.
29 J. A. Platts, S. P. Oldfield, M. M. Reif, A. Palmucci, E. Gabano and D. Osella, *J. Inorg. Biochem.*, 2006, **100**, 1199–1207.
30 *Virtual Computational Chemistry Laboratory* (VCCLAB), http://www.vcclab.org. See also: I. V. Tetko, J. Gasteiger, R. Todeschini, A. Mauri, D. Livingstone, P. Ertl, V. A. Palyulin, E. V. Radchenko, N. S. Zefirov, A. S. Makarenko, V. Y. Tanchuk and V. V. Prokopenko, *J. Comput.-Aided Mol. Des.*, 2005, **19**, 453–463.
31 G. Caron, G. Ermondi, M. B. Gariboldi, E. Monti, E. Gabano, M. Ravera and D. Osella, *ChemMedChem*, 2009, **4**, 1677–1685.
32 R. Mannhold and C. Ostermann, in *Molecular Drug Properties. Measurement and Prediction*, ed. R. Mannhold, Wiley-VCH, Weinheim, 2008, pp. 357–379.
33 (*a*) M. J. Cleare and J. D. Hoeschele, *Platinum Met. Rev.*, 1973, **17**, 2–13; (*b*) M. J. Cleare and J. D. Hoeschele, *Bioinorg. Chem.*, 1973, **2**, 187–210; (*c*) M. J. Cleare, *Coord. Chem. Rev.*, 1974, **12**, 349–405.
34 (*a*) M. Milanesio, E. Monti, M. B. Gariboldi, E. Gabano, M. Ravera and D. Osella, *Inorg. Chim. Acta*, 2008, **361**, 2803–2814; (*b*) E. Monti, M. Gariboldi, A. Maiocchi, E. Marengo, C. Cassino, E. Gabano and D. Osella, *J. Med. Chem.*, 2005, **48**, 857–866.
35 N. Farrell, Y. Qu, L. Feng and B. Van Houten, *Biochemistry*, 1990, **29**, 9522–9531.
36 (*a*) L. S. Hollis, W. I. Sundquist, J. N. Burstyn, W. J. Heiger–Bernays, S. F. Hellem, K. J. Ahmed, A. R. Amundsen, E. W. Stern and S. J. Lippard, *Cancer Res.*, 1991, **51**, 1866–1875; (*b*) L. S. Hollis, A. R. Amundsen and E. W. Stern, *J. Med. Chem.*, 1989, **32**, 128–136.
37 K. S. Lovejoy, R. C. Todd, S. Zhang, M. S. McCormick, J. A. D'Aquino, J. T. Reardon, A. Sancar, K. M. Giacomini and S. J. Lippard, *Proc. Natl. Acad. Sci. U. S. A.*, 2008, **105**, 8902–8907.
38 C. P. Anderson, J. M. Tsai, W. E. Meek, R. M. Liu, Y. Tang, H. J. Forman and C. P. Reynolds, *Exp. Cell Res.*, 1999, **246**, 183–192.
39 B. A. J. Jansen, J. Brouwer and J. Reedijk, *J. Inorg. Biochem.*, 2002, **89**, 197–202.
40 (*a*) F. I. Raynaud, F. E. Boxall, P. M. Goddard, M. Valenti, M. Jones, B. A. Murrer, M. J. Abrams and L. R. Kelland, *Clin. Cancer Res.*, 1997, **3**, 2063–2074; (*b*) J. F. Holford, F. I. Raynaud, B. A. Murrer, K. Grimaldi, J. A. Hartley, M. J. Abrams and L. R. Kelland, *Anti–Cancer Drug Des.*, 1998, **13**, 1–18; (*c*) Y. Chen, Z. Guo, S. Parsons and P. J. Sadler, *Chem.–Eur. J.*, 1998, **4**, 672–676.
41 E. Lindauer and E. Holler, *Biochem. Pharmacol.*, 1996, **52**, 7–14.
42 M. D. Hall, M. Okabe, D.-W. Shen, X. J. Liang and M. M. Gottesman, *Annu. Rev. Pharmacol.*, 2008, **48**, 495–535.
43 B. E. Bowler, L. S. Hollis and S. J. Lippard, *J. Am. Chem. Soc.*, 1984, **106**, 6102–6104.
44 G. L. Cohen, W. R. Bauer, J. K. Barton and S. J. Lippard, *Science*, 1979, **203**, 1015–1016.
45 Y. N. Kukushkin, Y. E. Vyaz'menkii, L. I. Zorina and Y. L. Pazukhina, *Zh. Neorg. Khim.*, 1968, **13**, 1595.
46 *SADABS*, *Area-Detector Absorption Correction*, Bruker AXS Inc., Madison, WI, 2004.
47 *SAINT*, *Area-Detector Integration Software* (*Version 7.23*), Bruker AXS Inc., Madison, WI, 2004.
48 A. Altomare, M. C. Burla, M. Camalli, G. Cascarano, G. Giacovazzo, A. Guagliardi, A. G. G. Moliterini, G. Polidoro and R. J. Spagna, *J. Appl. Crystallogr.*, 1999, **32**, 115–119.
49 G. M. Sheldrick, *SHELXL-97: Program for the Refinement of Crystal Structure*, University of Gottingen, Germany, 1997.
50 L. J. Farrugia, *J. Appl. Crystallogr.*, 1999, **32**, 837–838.
51 L. J. Farrugia, *J. Appl. Crystallogr.*, 1997, **30**, 565.
52 O. Heudi, S. Mercier–Jobard, A. Cailleux and P. Allain, *Biopharm. Drug Dispos.*, 1999, **20**, 107–116.
53 M. C. Alley, D. A. Scudiero, A. Monks, M. L. Hursey, M. J. Czerwinski, D. L. Fine, B. J. Abbott, J. G. Mayo, R. H. Shoemaker and M. R. Boyd, *Cancer Res.*, 1988, **48**, 589–601.
54 E. Gabano, D. Colangelo, A. R. Ghezzi and D. Osella, *J. Inorg. Biochem.*, 2008, **102**, 629–635.

